

Results from the Stanford 10 m Sagnac interferometer

Peter T Beyersdorf, Robert L Byer and Martin M Fejer

Ginzton Laboratory, Stanford University Stanford, CA 94305-4085, USA

Received 29 October 2001, in final form 18 January 2002

Published 14 March 2002

Online at stacks.iop.org/CQG/19/1585

Abstract

The design of a 10 m all-reflective prototype Sagnac interferometer with suspended optics is described and the experimental results are presented. It uses a polarization scheme to allow detection of the dark fringe on the symmetric port of the beamsplitter for optimal interference contrast. The necessary low-frequency response of the interferometer requires delay lines in the arms. To deal with the noise introduced by scattered light in the delay lines, a laser frequency sweep frequency shifts the scattered light so that it does not produce noise near zero frequency. This results in a shot-noise-limited phase sensitivity of $\Delta\phi = 1.6 \times 10^{-9}$ rad Hz^{-1/2} at frequencies as low as 200 Hz. Scaling this prototype to several kilometres with kilowatts of circulating power requires several technical improvements in high-power solid-state lasers, second harmonic generation and the fabrication of large mirrors, which are likely to be made in the next 10 years.

PACS number: 0480N

1. Introduction

Advanced gravitational wave detectors will require many kilowatts of circulating laser power. With such high circulating power the optics of the interferometer absorb a significant amount of heat leading to thermal distortions that limit the power in the desired mode of the interferometer [1]. For advanced gravitational wave detectors such as advanced LIGO [2] and the LCGT [3], the interferometer optics will either need adaptive compensation of thermal distortions [4] or will need to be used only in reflection.

Table-top experiments have demonstrated a Sagnac interferometer with many of the characteristics necessary for an advanced gravitational wave detector [5–7]. Here I present the first prototype Sagnac interferometer with all-reflective suspended optics and a 10 m delay line that incorporates the design elements already proven by table-top experiments, specifically the use of all-reflective optics, external modulation and a polarization scheme to allow detection of the dark fringe on the symmetric port of the beamsplitter. The interferometer design is highly insensitive to thermal distortions because of the lack of transmissive optics and does not need to be actively controlled because of the relative phase stability of the interfering

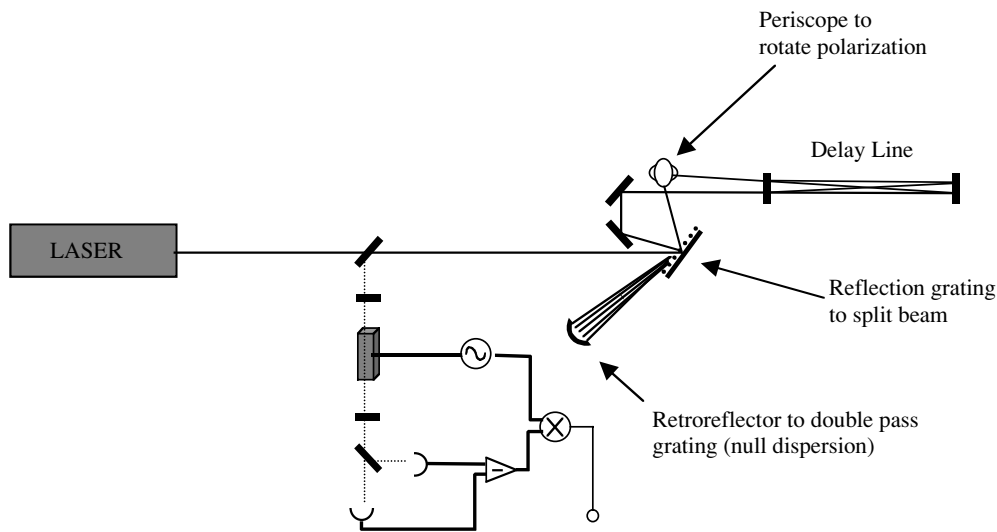


Figure 1. The 10 m polarization delay-line Sagnac interferometer. The laser is split by the reflection grating. The diffracted beam is re-imaged onto the grating by a retro-reflector before travelling around the interferometer loop. The beams travel in opposite directions around a common path including 49 round trips between the delay line mirrors and through the periscope which rotates the polarization by 90° . The beams are re-combined by the grating and propagate back towards the laser where the dark fringe polarization is separated by a polarizing beamsplitter for signal read-out (dotted line). For signal read-out via heterodyne detection, a modulator adds local oscillator sidebands before the balanced detectors.

beams inherent in common path interferometers. To reduce the effect of scattered light noise in the delay lines a laser frequency sweep is used that frequency-shifts the scattered light noise spectrum. The interferometer sensitivity was shot-noise-limited above 200 Hz with a phase sensitivity of 1.6×10^{-9} rad $\text{Hz}^{-1/2}$.

2. Interferometer design

Key elements of the all-reflective Sagnac interferometer are shown in figure 1. Included is the reflective grating beamsplitter, the delay-line mirrors and the optics used for polarization control. A reflection grating with one reflected order and one diffracted order is used as the beamsplitter. The diffraction efficiency is highly polarization dependent so the grating functions like a polarization beamsplitter. A mirror with a 500 mm radius of curvature is located 1 focal length from the diffraction grating to re-image the diffracted beam onto the grating, displaced slightly in the vertical plane from the incident spot. By re-imaging the beam onto the grating the influence of the grating on the beam is compensated; the ellipticity of the diffracted beam produced by the first diffraction is corrected by the second, and the variation in angle that is produced by fluctuations in the laser frequency, or by variations in the grating pitch (such as those produced by thermal distortions), is removed.

Polarization control in the Sagnac interferometer allows the dark fringe to be observed on the symmetric port of the beamsplitter, maximizing the interference contrast. The grating splits the light by polarization, so an element that rotates the polarization of the circulating light by 90° causes the diffracted beam to be reflected upon returning to the beamsplitter and the reflected light to be diffracted, ensuring that imperfections of the beamsplitter affect both

beams equally. A periscope is used to rotate the polarization of the light. Since the geometry of the periscope rotates the entire spatial profile of the beam, the polarization is also rotated. Although this element is conceptually simple to understand, it complicates the alignment of the interferometer by coupling the vertical alignment of one of the interfering beams to the horizontal alignment of the other.

The delay line mirrors are 6 inch diameter silicon substrates from General Optics polished and coated to have a reflectivity of 0.9999. The mirrors have a 10 m radius of curvature and are placed slightly less than 10 m apart so as to have 49 round trips of the light before the input beam is re-imaged onto itself. The circular pattern of beam spots on the mirrors has a 3 inch diameter. The input beam is tightly focused onto a thin (1 mm \times 25 mm) mirror, placed just in front of the reflecting surface of one delay line mirror. The input beam reflects off this thin mirror while the neighbouring beam spots are just above and below.

The delay line mirrors are each held in an aluminium cradle, suspended from a tip-tilt plate mounted on a unistrut frame inside the Engineering Test Facility vacuum chamber at Stanford University. The suspension consists of five splayed wires in two parallel planes intended to constrain the motion of the mirror for all degrees of freedom except the longitudinal translational motion. The longitudinal motion has a resonant frequency of 1 Hz and a seismically driven rms amplitude of 50 μ m. The yaw degree of freedom for the mirror is quite soft with a resonant frequency of about 1.5 Hz but is efficiently damped by eddy current damping from magnets mounted on the unistrut frame near the ends of the suspension cradle so as to preferentially damp the yaw motion. All other degrees of freedom had resonant frequencies above 10 Hz. All other components in the interferometer loop including the grating beamsplitter, and steering mirrors were mounted on a single aluminium breadboard which was itself suspended from the unistrut frame in the vacuum system by a five-wire suspension. The motion of the breadboard was predominantly in the longitudinal direction with a resonant frequency of 1 Hz. Its motion was not damped because unlike the other less massive suspension systems, large motions of the breadboard were not typically excited during manual alignment of the optics. All other degrees of freedom were relatively stiff with resonant frequencies above 10 Hz.

The delay line mirrors have high reflectivity to minimize the loss of the beam folded between them. There is also, however, very low loss for scattered light that gets trapped in a cavity mode. This scattered light can acquire an arbitrary phase and scatter back into the path of the delay line beam. This degrades the common-mode noise rejection of the system introducing sensitivity to technical laser noise and allowing large out-of-band seismic noise to up-convert into the measurement band. To reduce the effects of the scattered light noise, a laser frequency chirp is used. The laser crystal temperature is slowly varied with a triangular waveform so that the laser frequency sweeps over 5 GHz with a 10 s period. With the frequency of the detected light a function of time, the scattered light that reaches the photodetector, having been in the interferometer for a different amount of time to the main beam (at least long enough for one round trip between the interferometer mirrors), has a frequency difference from the main beam. The noise from the scattered light is thus shifted by the beat frequency, set to be outside the measurement band.

Light enters and exits the vacuum chamber through a quartz window on the vacuum flange. Outside the chamber a polarization beamsplitter separates the dark fringe of the light returning from the beamsplitter from the orthogonally polarized bright fringe which propagates back towards the laser unused. A portion of the light in the orthogonal polarization is modulated at 96 MHz and mixed with the dark fringe on a pair of balanced detectors. A quarter-wave plate removes the phase difference between the 96 MHz local oscillator and the dark fringe and a half-wave plate and polarizer project the sum of the local oscillator and the dark fringe

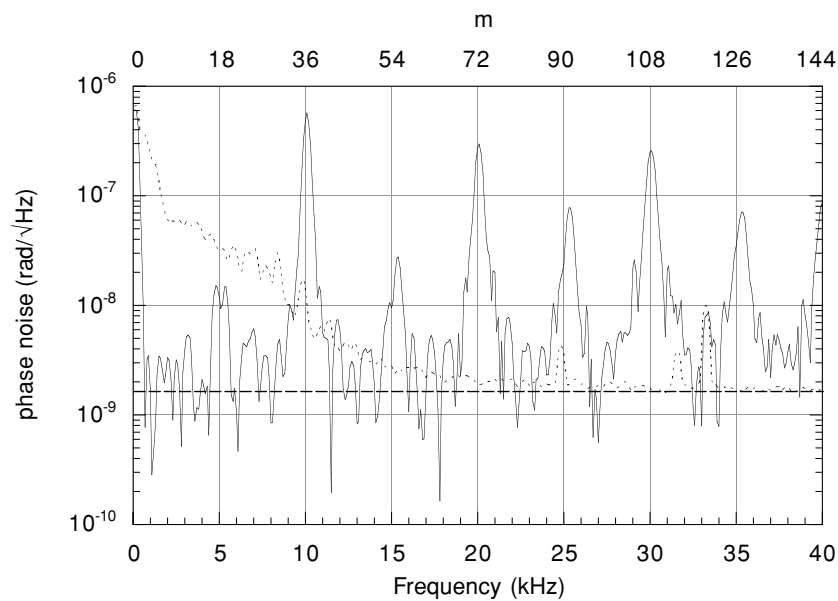


Figure 2. The noise spectrum of the interferometer. Without a laser frequency chirp (dotted curve) the sensitivity is limited by scattered light noise below 20 kHz. With the laser frequency chirp (solid curve) the scattered light noise is frequency shifted (to the many peaks spaced 5 kHz apart) and the sensitivity from 200 Hz to 5 kHz is limited by the shot-noise (dashed line) from 150 mW of light.

onto one detector and the difference of the two beams onto the other. The photocurrents of the two photodiodes are converted to voltage by a transimpedance amplifier and the voltages are subtracted and demodulated at 96 MHz.

3. Experimental results

The sensitivity of the interferometer below 20 kHz was limited by scattered light noise when the laser frequency chirp was not used. Above 20 kHz the sensitivity was shot-noise limited for 150 mW of detected laser power. With the laser frequency chirp, scattered light noise was shifted above 5 kHz, allowing shot-noise-limited sensitivity from 200 Hz to 5 kHz. Figure 2 shows the noise level from 0 to 40 kHz so that the frequency-shifted scattered light noise due to the laser frequency chirp can be clearly seen; however, with this entire frequency range plotted the 200 Hz low frequency limit for shot-noise-limited operation is not resolvable. Since this prototype contains only a single arm, it is not appropriate to convert the phase sensitivity to displacement sensitivity for this configuration.

The operation of the interferometer is quite robust due to the inherent stability of common-path interferometers. The interferometer is operational for days at a time before the slow drift of the optics requires the beams to be realigned via a pair of motorized mirror mounts in the interferometer loop. A phase sensitivity of 1.6×10^{-9} rad Hz^{-1/2} was demonstrated even in the presence of the 50 μ m rms motion of the mirrors.

The reflective grating beamsplitter, together with the retro-reflecting mirror to compensate grating dispersion and beam shaping, allows the alignment of the beams to be maintained in

the presence of the large laser frequency variation due to the chirp used to reduce scattered light noise.

4. Conclusion

The 10 m suspended polarization delay-line Sagnac interferometer demonstrated an interferometer topology useful for advanced gravitational wave detectors where high circulating power is required. There are three key components to this design. The first is a polarization scheme, using a reflection grating with the diffracted beam re-imaged on the grating, to split and recombine the beams and a reflective periscope to rotate the polarization of the circulating light. This scheme allows the interference contrast to be maximized for the dark interference fringe.

The second key component is the signal read-out scheme. The dark fringe and the bright fringe of the interferometer are collinear but orthogonally polarized. The bright fringe is used as a local oscillator by manipulating its phase and frequency relative to the dark fringe through polarization sensitive waveplates and modulators at the output of the interferometer where the optics are not subject to the high input power. A balanced detection system combines the signal and local oscillator so that the output has little sensitivity to laser amplitude and technical frequency noise.

The final key to the interferometer design is the laser frequency sweep to reduce the in-band noise from the scattered light. Scattered light from the delay lines that reach the photodetector is frequency shifted from the main beam because of the laser frequency chirp and the time delay between the scattered light and the main beam. A properly tailored chirp results in the scattered light noise being shifted outside of the measurement band.

Scaling this prototype to several kilometres with kilowatts of circulating power requires various technical improvements. High-power solid-state lasers will be required since the all-reflective design does not lend itself to the use of power recycling. Additionally, it will be necessary to use non-linear optics to generate shorter wavelength light (than the fundamental wavelength of Nd:YAG lasers) to allow the many round trips in the delay line that are necessary for tuning the interferometer response below 1 kHz in a kilometre-scale interferometer. The 1 m diameter delay line mirrors necessary to accommodate the many reflection spots also present a technical manufacturing challenge and the photothermal noise [8] in the delay line mirrors must be understood and possibly addressed. If these challenges can be met, a scaled-up version of this Sagnac interferometer may be used in an advanced gravitational wave detector with high circulating power.

References

- [1] Hello P and Vinet J Y 1990 *J. Phys., France* **51** 1276–82
- [2] Gustafson E, Shoemaker D, Strain K and Weiss R 1999 LSC White Paper on detector research and development *Technical Report LIGO-T990080* (LIGO Project/California Institute of Technology)
- [3] Kuroda K and the LCGT Collaboration 1999 *Int. J. Mod. Phys. D* **8** 557–79
- [4] Marfuta P 2001 Testing dynamic thermal compensation of optics for use in LIGO II *BSc Thesis* MIT
- [5] Traeger S, Beyersdorf P T, Goddard L and Gustafson E K 2000 Polarization Sagnac interferometer with a reflective grating beam splitter *Opt. Lett.* **25** 722
- [6] Beyersdorf P T, Fejer M M and Byer R L 1999 Polarization Sagnac interferometer with postmodulation for gravitational-wave detection *Opt. Lett.* **24** 1112
- [7] Beyersdorf P T, Fejer M M and Byer R L 1999 Polarization Sagnac interferometer with a common-path local oscillator for heterodyne detection *J. Opt. Soc. Am. B* **16** 1354
- [8] Braginsky V B, Gorodetsky M L and Vyatchanin S P 1999 Thermodynamical fluctuations and photo-thermal shot noise in gravitational wave antennae *Phys. Lett. A* **264** 1–10